TITLE: HDAC3 inhibition harnesses learning-induced neurobiological mechanisms to enhance signal-in-noise responsivity in auditory cortex and behavior

ABBREVIATED: Learning modulates cortical coding of signals in noise

Nilay Ateşyakar[1,2] and Kasia M. Bieszczad*[1,2,3]

Authors Affiliations:

1. **Department of Psychology—Behavioral and Systems Neuroscience, Rutgers University, Piscataway, NJ, 08854, USA**
   Nilay Ateşyakar & Kasia M. Bieszczad
2. **Rutgers Center for Cognitive Science (RuCCS), Rutgers University**
   Kasia M. Bieszczad
3. **Department of Head & Neck Surgery and Communication Sciences, Rutgers Robert Wood Johnson Medical School, New Brunswick, NJ, 08901, USA**
   Kasia M. Bieszczad

***Corresponding author:**

Correspondence to Dr. Kasia M. Bieszczad
327 Psychology Building, Rutgers University-New Brunswick
152 Frelinghuysen Road
Piscataway, New Jersey 08854 USA
kasia.bie@rutgers.edu

Number of pages: 32

Number of figures and tables: 6 Figures / 3 additional Supplemental Figures

Number of words: Abstract – 251; Introduction – 772; Discussion –1829

Conflict of interest statement: The authors declare no competing financial interests.

Acknowledgements: This work was supported by the National Institutes of Health, the National Institute on Deafness and Communication Disorders [R01-DC018561 to K.M.B.] and funding from the School of Arts and Sciences at Rutgers University—New Brunswick. The authors wish to thank Dr. Justin Yao for helpful discussions that motivated analyses that contributed to the completion of this work. We also thank all former and current members of the CLEF Lab, especially Dr. Andrea Shang, who generated initial versions of the analytical code that was adapted for investigating auditory cortical response profiles across noise conditions; and to Rebecca Shear, who contributed to animal training across the large cohort reported, and to Elias Youssef who offered technical assistance throughout the project. The authors are also grateful to the membership of Rutgers Auditory Neuroscience Research Initiative (RANRI) for their continuous insight and valuable input to this project.

ABSTRACT

Auditory learning enables sound-guided behavior and sound-specific enhancements in auditory cortical (AC) processing. Background noise can also alter sound-specific auditory responsivity. Yet, the potential enhancing effects of learning on AC processing in noise is unknown. Pharmacological inhibition of histone deacetylase 3 (HDAC3) by RGFP966 has been shown to improve AC coding when administered during various auditory learning paradigms. Here, adult rats (Sprague-Dawley males) were trained in ideal quiet conditions to learn a tone-reward associative task while treated with RGFP966 (TRAINED+RGFP966, n = 6) to determine if learning-related effects on AC could support tone-signal detection in a later background noise challenge. RGFP966 accelerated sound-reward learning relative to a trained but untreated group of rats (TRAINED, n = 5), though all animals ultimately reached equivalent high levels of performance prior to testing. Training produced a *sound-specific* enhancement in AC responses evoked by the signal tone, and a *sound-general* effect that suppressed responses during steady-state noise, relative to untrained rats (NAÏVE, n = 7). Effects were strongest when training was with RGFP966 administration and scaled with increasing signal-to-noise (SNR). High levels of background noise abolished sound-specific enhancements in tone-signal evoked AC activity, yet the general suppressive effect to noise was maintained. Remarkably, behavioral responses to the signal tone in different SNRs recapitulated AC patterns of tone-evoked responding. Overall, rapid auditory learning facilitated by RGFP966 yields AC plasticity that can improve signal detection. Learning-induced mechanisms appear to shape cortical decoding mechanisms that selectively enhance representations of signal sounds and suppress the effects of background noise.

SIGNIFICANCE STATEMENT

Difficulty hearing in noise is a widespread challenge, yet the cortical mechanisms that preserve meaningful sounds under noisy listening conditions remain unclear. We show that HDAC3 inhibition accelerates auditory learning and strengthens cortical encoding of a learned tone while suppressing background noise activity in ways that predict improved behavioral detection. These findings reveal an experience-driven cortical mechanism that supports improved hearing in challenging listening environments, which may inform strategies for enhancing auditory learning and rehabilitation using HDAC3 drug-targets.

INTRODUCTION

A major function of the auditory system is to identify behaviorally relevant acoustic signals in the presence of competing background noise. Successful sound-guided performance depends on neural mechanisms that enhance the fidelity and selectivity of sound representations beyond what can be explained by peripheral signal-to-noise ratio (SNR) alone. Experience like associative learning drives plasticity in the auditory cortex (AC), producing lasting modifications to receptive field tuning, excitatory–inhibitory circuit balance, and population-level coding, including tonotopic organization (Weinberger, 2004; Schreiner and Polley, 2014; Froemke, 2015). Learning-induced changes enhance encoding of behaviorally relevant sounds (Fritz et al., 2003) and contribute to the formation of precise auditory memories (Bieszczad and Weinberger, 2010; McGann, 2015). However, it remains unknown how learning-driven changes in cortical coding support sound-guided behavior under degraded listening conditions such as background noise.

Background noise alters AC responses that directly affect auditory discrimination (Alain et al., 2014). Noise increases the sound levels required for tone-evoked activity and decreases response magnitudes (Phillips, 1985; Phillips and Hall, 1986). Human word recognition declines with increasing noise even when SNR is held constant (Studebaker et al., 1999; Dubno et al., 2005). In animal models, noise reduces neural population response diversity (Shilling-Scrivo et al., 2021) and modulates tuning selectivity in an SNR- and level-dependent manner (Teschner et al., 2016). Yet in some cases, noise can enhance discrimination of closely spaced frequencies by reducing overlap among cortical tuning curves (Christensen et al., 2019). Cortical inhibition plays a central role in regulating receptive field structure during both passive and learning-dependent conditions (Lakunina et al., 2022). For example, activating parvalbumin-expressing interneurons can mimic noise-induced reductions in responsivity and enhance discrimination of spectrally similar tones (Christensen et al., 2019; Nocon et al., 2023). Inhibitory circuits also contribute to the formation and maintenance of learning-induced AC plasticity and to the consolidation of long-lasting auditory memories (Aizenberg et al., 2015; Blackwell and Geffen, 2017; Natan et al., 2017; Wood et al., 2017; Lakunina et al., 2022; Studer and Barkat, 2022). These findings support the view that experience-dependent changes to receptive field tuning, threshold, and excitatory–inhibitory structure, strongly influence the capacity to separate tone signals from noise at both neural and behavioral levels. Learning-induced receptive field plasticity in AC may therefore provide a mechanistic substrate for improved signal-in-noise performance. Although receptive field plasticity can adaptively shape frequency-specific AC responses during learning, long-lasting improvements in signal processing likely require molecular processes that reliably stabilize these changes.

Epigenetic processes—including histone acetylation and DNA methylation—provide a mechanistic route for regulating molecular programs required for long-term memory consolidation (Shang and Bieszczad, 2022) that can effectively set the threshold for memory formation (Phan and Bieszczad, 2016). Epigenetic modulation shapes experience-dependent sensory cortical plasticity in ways that strongly influence the selectivity of sensory signals encoded in memory and can support unusually persistent memories (Stefanko et al., 2009). Among epigenetic targets, histone deacetylase 3 (HDAC3) has shown particularly selective effects on auditory cortical plasticity (Bieszczad et al., 2015). For example, HDAC3 inhibition during auditory associative learning enhances frequency-specific tuning changes and expands tonotopic map regions that

represent the signal frequency, relative to identically trained untreated animals (Shang et al., 2019; Rotondo and Bieszczad, 2020, 2021a, 2021b). Remarkably, neurophysiological effects correspond to sharply frequency-specific behavioral responding in memory tests and persist for weeks. Treatment may help to encode and stabilize precise acoustic details of the learned signal, which underscores a novel potential for HDAC3 inhibition to promote long-lasting effects on listening abilities via molecular genetic control on cellular function (Graham et al., 2023). HDAC3 inhibition may similarly promote signal-specific AC responses in novel background noise by creating an *a priori* advantage for processing a learned sound signal. Likewise, while HDAC3 inhibition reliably increases behavioral memory specificity in silent backgrounds, its ability to guide sound-selective behavioral performance in novel noisy environments remains unexplored. Further, by its action to selectively enhance the consolidation of frequency-specific learning, HDAC3 manipulations may reveal the neural coding features in AC that optimize accurate signal-in-noise detection. Identifying how outcomes of HDAC3-regulated auditory learning interact with noise-driven modulation of AC tuning will therefore help delineate the neurobiological substrates that support listening skills and their dependence on experience-dependent cortical plasticity.

The present study aims to determine how memory specificity for a learned acoustic signal is expressed behaviorally and cortically in the presence of background noise, and whether HDAC3 inhibition can enhance these processes. Understanding how learning-induced plasticity interacts with noise-dependent dynamics in AC will advance our understanding of the neurobiological mechanisms that support sound-guided behavior under natural listening conditions. Indeed, despite its relevance to real-world listening, the neural expression of learned sounds in backgrounds of noise has been understudied.

MATERIALS AND METHODS

Subjects: Adult male Sprague Dawley rats weighing 250-300 grams on arrival served as subjects in this experiment in 3 groups: (1) TRAINED, n=15; (2) TRAINED+RGFP966, n=10; and (3) NAÏVE, n=7. Animals that were to undergo training were water-restricted and maintained at 85% of the free-drinking weight of littermate controls for the duration of training and memory testing. Untrained rats (the NAÏVE group) were never water restricted. Water supplementation was administered as needed to maintain weight and was given *ad libitum* prior to any surgical procedures. All rats were handled daily by an experimenter after arrival to the laboratory for at least 5 days before beginning any other procedures to acclimate animal subjects to transport to the lab, experimental handling, and the ambient sounds of the laboratory. The vivarium maintained a 12:12 light/dark cycle (lights on at 7am; lights off at 7pm). All procedures were approved and conducted in accordance with guidelines by the Institutional Animal Care and Use Committee at Rutgers, The State University of New Jersey (#PROTO999900026 to K.M.B.), in accordance with relevant named guidelines and regulations, and are reported in compliance with ARRIVE guidelines.

Behavioral Training. Behavioral sessions were conducted in three identical instrumental conditioning chambers (Habitest Modular Test Cage System, 12”x10”x12” chamber; this and all Habitest modular components were from Coulbourn Instruments, Lehigh PA) fitted with a bar floor

(H10-11R-TC-SF) within a custom-built sound-attenuating box. Each chamber was fitted with a response lever (H21-03R), house light (H11-01R), infrared lights (H27-91R), speaker (H12-01R) and a water delivery system (H14-05R) along the same wall. When triggered either by the response lever or a hand switch (H21-01), the water delivery system would present a water cup (0.1cc of water) in the reward port (1.26" W x 1.625"H). Daily training sessions were counterbalanced to ensure equal exposure to different chambers. All behavioral protocols were created in and run using Graphic State 4 software. Behavioral responses were recorded at a resolution of 1 millisecond. Auditory stimuli were generated using Tucker-Davis Technologies (TDT) hardware (RZ6) and RPvdsEx software (TDT; Alachua, FL) at a 50 kHz sampling rate and presented via the operant chamber's wall-mounted speaker.

Rats were first behaviorally shaped to lever press for water rewards (1:1 fixed ratio) in daily 45-minute sessions across five consecutive days. Twenty-four hours following successful shaping in which animals independently initiated and maintained bar-press responding for water rewards across the 45-minute session or to satiation, animals began daily training sessions on a tone-reward associative learning task. During each 45-minute training session, tone trials were presented such that on each trial, animals heard a 5.0-kHz pure tone (60 dB SPL; 8 sec) and any lever presses made during the tone duration were reinforced with water reward (3 second access to the water delivery dipper system). Responses during silent inter-trial intervals (ITI; range: 5–25 seconds, randomized) resulted in an error signal (flashing house light) and a "time-out" a flashing house light error signal that initiated a 6-second time-out period that delayed the time until the next tone trial. Task acquisition was evaluated using two complementary performance criteria: First, an 80% performance criterion was defined as the first day on which the session performance (performance = [lever presses during tones / all bar presses during session] x 100) exceeded 80% and remained above 80% on the following day of tone-reward training. This metric was used to quantify learning speed. Second, asymptotic performance was defined using more stringent stability-based criteria to ensure high levels of stable performance prior to memory testing and electrophysiological recording: (1) a performance exceeding 90% on at least two of the last three training days within a maximum of 20 training days, and (2) performance stability, measured as a coefficient of variation below 10% across the final five training days. Animals proceeded to memory testing only after reaching asymptotic performance, or after >20 sessions of daily training. This performance criterion ensured stable, high-level task performance at the time of evaluating memory specificity and later electrophysiological recording in AC. Only 1 animal (from the TREATED group) failed to achieve this performance criterion, so training was halted after 20 daily sessions of tone-reward task training.

Pharmacological HDAC3 inhibition via RGFP966. To examine the role of HDAC3 inhibition in auditory learning, a subset of animals that comprised the TRAINED+RGFP966 group received systemic post-training injections of the selective HDAC3 inhibitor, RGFP966 (10 mg/kg, subcutaneous; ApexBio #A8803) immediately following training sessions on days 2, 3 and 4. Animals that were to undergo injections were exposed to the same handling procedure used to perform the injections for at least 5 days prior to injections (e.g., immediately following bar-press shaping sessions and after the first daily session (day 1) of tone-reward training) to reduce effects of novelty or arousal that later could have been induced by the injection itself. Trained animals that were not injected with RGFP966 (the TRAINED group) included animals that received either

vehicle injections (equivalent volume, subcutaneous) immediately after training sessions on days 2, 3 and 4; or no injections at all across training. Vehicle injections did not produce differences in task acquisition in animals that were not injected (Wilcoxon rank-sum test: W=30.5, p=0.72; mean day to reach 80%; **Fig. S1**), so these animals were collapsed into a single (TRAINED) group. That injections themselves did not alter task performance is important to reinforce that any effects of injecting RGFP966 were due to the effects of the HDAC3 inhibitor itself, and not confounded by indirect effects of experiencing a subcutaneous injection.

Memory Test. Upon meeting the performance criteria, a behavioral memory test was conducted to assess individual differences in noise-sensitive and frequency-selective behavior. To ensure stable task performance immediately prior to the Memory Test, animals completed a brief version of the tone–reward task, which lasted approximately 5 minutes (mean = 4 min 52 sec ± 29 sec). This brief session also served as a warm-up that was immediately followed by the Memory Test. Each animal received 117 pseudorandomized trials (three blocks of 39) in which the a single tone was presented (8 sec) at either the signal frequency (5.0 kHz) or ±¼ octave away at two nearby novel frequencies (4.2 and 5.9 kHz). Intertrial intervals were variable (5–20 sec). Tone presentations during the Memory Test were not reinforced with water rewards. Tones were delivered either in Quiet or embedded in notched white noise at three levels that produced a defined signal-to-noise ratio: low noise (60 dB tone + 20 dB noise; SNR40), medium noise (60 dB tone + 40 dB noise; SNR20), and high noise (60 dB tone + 60 dB noise; SNR0, see **Fig. S2**). Noise was Gaussian white noise regenerated from a normal distribution on every trial (frequency range <25kHz; gated with 20 ms cosine rise/fall ramps). The notch filter was introduced at the frequency of the tone embedded in noise on every single trial to ensure that animals could not use an increase in spectral energy with frequency channels to guide their sound-cued behavior. As such, bar-presses during tone presentations were interpreted to be driven by activating an internal representation of the learned association between a specific tone frequency and the availability of reward.

Noise-sensitive and frequency-selective behavioral performance was analyzed separately for each noise condition within individual subjects before determining group-level effects. For each noise level, frequency-selective responding was quantified as the percentage of bar presses made during tone presentations to a given frequency relative to the total number of bar presses made during tone presentations of all frequencies tested within the same noise condition. This was, computed as: Proportion of Bar Presses % = (total # of bar presses made during tone A / total # of bar presses made during any tone at that SNR) × 100.

Finally, to ensure that the unrewarded context of memory testing did not catastrophically disrupt performance prior to electrophysiological recording, all animals went through a final task session of the tone-reward learning paradigm 24-48 hours later to confirm maintained task performance. All animals maintained performance from the last training session prior to memory testing ($t(10) = 0.92$, $p = 0.37$; paired samples t-test; **Fig. S3A**). Further, the final performance level measured after memory testing did not differ between groups ($t(9) = 1.13$, $p = 0.28$; independent samples t-test; **Fig. S3B**), which indicated that RGFP966 did not produce any effects on the maintenance of task performance following the memory testing session.

Surgical Procedures. Following behavioral testing, *in vivo* multiunit electrophysiological recordings targeting auditory cortex (AC) were performed. All surgical procedures were conducted in a custom designed double-walled, walk-in sound-attenuated chamber (Industrial Acoustics Co., Bronx, NY). Animals were anesthetized with sodium pentobarbital (60 mg/kg, i.p.), with supplemental doses (10-15 mg/kg, i.p.) administered as needed to maintain a surgical plane of anesthesia. Atropine methyl nitrate (10 mg/kg, i.m.) was administered to minimize bronchial secretions. Ophthalmic ointment (Puralube®) was applied to prevent corneal desiccation. Core body temperature was maintained near 36–37°C throughout the procedure using a heating pad closed-loop homoeothermic warming system, continuously monitored via a rectal temperature probe (TC-1000, CWE Inc.). While under anesthesia, the head was shaved to reveal the scalp and the animal was mounted in a modified stereotaxic frame that tilted to provide access to the temporal plane (Kopf Instruments, Tujunga, CA). To provide local anesthesia, 2% lidocaine (LidoJect; Henry Schein; ~1 mL, s.c.) was administered in small boluses across the scalp. The scalp was then resected, and the skull was secured to a head holder using several small stainless-steel screws and dental acrylic. This fixation allowed removal of the ear bars while maintaining the head in a stable and fixed position for the duration of the procedure. Animals were then secured in a stereotaxic apparatus. The right temporal muscle was retracted to expose the skull overlying auditory cortex. A craniotomy was performed over the right temporal cortex, and the dura mater was carefully removed to expose the cortical surface, which was maintained using warm sterile 0.9% saline application throughout the cortical mapping procedure to prevent cortical desiccation. The cisterna magna was periodically drained of cerebrospinal fluid to reduce cerebral swelling and improve cortical stability as needed.

Auditory Cortical Mapping Procedures. To characterize the frequency-selective responsiveness of auditory cortical sites within the tonotopic organization primary auditory cortex (A1), animals underwent a terminal auditory cortical mapping procedure that followed established protocols described previously (Bieszczad & Weinberger, 2010a, 2010b, 2012; Bieszczad et al., 2015; Elias et al., 2015; Shang et al., 2019). Extracellular responses to acoustic stimuli were recorded across auditory cortex using parylene-coated tungsten microelectrode arrays consisting of six (2 × 3) channels (FHC, Bowdoin, ME; 1–2 MΩ impedance; 250 μm inter-electrode spacing). Electrodes were advanced orthogonal to the cortical surface into the thalamorecipient middle cortical layers (III–IV; approximately 400–600 μm depth) using a precision microdrive (IVM-1000; Scientifica, UK). Multiple penetrations (M=85.66 sites, SE=10.41 per animal in Phase 1; M=32.33 sites, SE=3.94 per animal in Phase 2; see Phase definitions in *Electrophysiological Recording Procedures*) were distributed across the cortical surface to obtain comprehensive spatial sampling of tone-responsive sites across the auditory cortex (AC). Photographs of the cortical surface were acquired prior to each penetration (OCS-SK2-14X; OptixCam Summit K2) to document electrode placement. Images were subsequently aligned using vascular landmarks to reconstruct a relative spatial map of recording sites and to delineate the borders within AC tonotopic organization.

Electrophysiological Recording Procedures. All acoustic stimuli were delivered monaurally to the contralateral (left) ear via a single calibrated electromagnetic speaker (MF1; Tucker-Davis Technologies Inc.) positioned approximately 10 cm from the ear canal. Recordings at each cortical site were conducted in two sequential phases. Trial structure and stimulus timing were adapted

from a previous study demonstrating the effects of background noise on auditory cortical frequency processing (Teschner et al., 2016).

Phase 1: In the first phase of the recording sequence, a search stimulus paradigm was used to confirm recording locations were bone fide sites within primary auditory cortex (A1) defined by short-latency responses to pure tones within the confines of the tonotopic organization of low to high frequencies from posterior to anterior locations across the temporal axis of the cortical plane. In this phase, tones were only presented in a Quiet background to assess short-latency, well-tuned frequency-selective responses characteristic of A1. Pure tones spanned a 0.525–47.700 kHz frequency range (in quarter-octave spacing; 25 ms duration gated with 5 ms cosine rise/fall ramps), presented pseudorandomly at sound levels ranging from 10 to 60 dB SPL (in 10-dB steps), with 6 repetitions of each of the 162 frequency-level stimuli. This generated 972 number of total trials across the recording that included 27 frequencies and 6 sound levels. Inter-stimulus intervals were randomly jittered between 585-865 ms in 52 ms steps.

Phase 2: If the recording site could be confirmed as A1, the second phase of the recording sequence would proceed. In this phase, tone-evoked responses were recorded under different SNR conditions. Tones were identical to the first phase frequency range 0.525-47.700 kHz (quarter octave steps, 25 ms duration gated with 5 ms cosine ramps) at 10-60 dB SPL (10 dB steps). However in this recording phase, acoustic stimuli could be embedded in white Gaussian noise (i.e., regenerated from a Gaussian distribution on every trial; frequency range <25kHz) presented at three defined and fixed signal-to-noise ratios. Pure tones were presented either in Quiet (SNR∞) or embedded in noise at fixed signal-to-noise ratios of low noise (SNR40) and high noise (SNR20). Each sound trial began with a pre-tone noise segment gated with 10 ms cosine ramps, followed by the onset of a 25 ms pure tone gated with 5 ms cosine rise/fall ramps that was effectively embedded within the noise duration. Noise continued for an additional 150 ms following tone offset. The onset latency of the tone relative to noise onset was at least 275 ms to generate a steady-state noise response, and varied pseudorandomly on different trials to be between 275 and 415 ms (in 20 ms increments). This generated a jitter so that tone onsets could not be predicted by the onset of the noise on each trial. Every trial concluded with a 275 ms silent interval to allow the system to return to an effective baseline, which ultimately yielded a fixed inter-noise interval of 725 ms from noise onset on one trial to the following trial noise onset. Each of the 162 frequency-level combination stimuli was pseudorandomly presented in 8 repetitions within each SNR condition for a total of 3888 trials across this phase of the recording session.

Neural signals were routed via a ZIF cable connecting the array adaptor mounted on the animal's head to a 16-channel analog headstage and amplifier (PZ5 NeuroDigitizer Amplifier; Tucker-Davis Technologies) located outside of the recording chamber. Signals were amplified (×1000), digitized at 24.414 kHz using RZ6-A-P1 and RZ5D BioAmp processors (Tucker-Davis Technologies), and stored for subsequent offline spike detection and analysis using custom MATLAB© scripts. Data collection and online stimulus presentation were controlled using Synapse™ software (Tucker-Davis Technologies). Neural activity was monitored in real time using TDT Synapse™ and OpenEx software to initially determine tone and frequency selectivity, and these data were also stored for subsequent offline analysis.

Offline, unfiltered recordings were digitally band-pass filtered between 300 and 3000 Hz to isolate multiunit activity relative to timestamps that indicated noise and tone onsets across the continuous time series data. When present, which was rare, line noise and its harmonics (60 Hz and multiple) were identified on a per-channel basis and attenuated prior to spike detection. Multiunit discharges were characterized using previously reported temporal and amplitude criteria (Elias et al., 2015). Briefly, spike detection was performed using a window-discrimination method. For each recording site, detection thresholds were defined relative to the root mean square (RMS) of the signal computed from 500 randomly selected traces. Positive and negative detection thresholds were set at 1.5×RMS and 2.0×RMS, respectively. Accepted spike waveforms were required to exhibit peak-to-peak separations of no more than 0.6 ms. Spike waveforms associated with large-amplitude transients exceeding predefined amplitude thresholds were excluded to minimize contamination by electrical or unexpected and rare movement-related artifacts.

For each recording site, tone-evoked firing rates (spikes/s) were calculated by subtracting activity measured during a 40 ms window immediately prior to tone onset (−40 to 0 ms, with 0 defined as tone onset) from tone-evoked spiking measured during a 40 ms response-onset window (6–46 ms following tone onset). Responses exceeding ±1.0 SEM of the pre-tone firing rate were classified as evoked. Tone-evoked activity was used to construct frequency-response areas (FRAs) for each recording site, representing mean sound-evoked activity across all frequency-intensity combinations.

A behaviorally untrained and pharmacologically untreated control group (NAÏVE; n = 7) underwent identical electrophysiological recording procedures to establish baseline auditory cortical response properties in the absence of experimental training or pharmacological treatment beyond experiences of experimenter handling and housing within a standard vivarium and laboratory environment. These data were included in group comparisons that were ultimately conducted between three groups: NAÏVE, TRAINED, TRAINED+RGFP966.

Frequency-selective AC Analyses. Analyses of frequency-selective effects in AC focused on activity evoked by the three behaviorally tested frequencies (4.2, 5.0, and 5.9 kHz) presented at either 60 or 40 dB SPL. To facilitate group-level comparisons across recording sites and experimental conditions, evoked firing rates were Z-scored within each signal-to-noise ratio condition. All analyses were performed using custom MATLAB© scripts. See *Results* for details.

Code Accessibility. Custom Matlab© scripts used to analyze behavioral and neurophysiological data within will be provided within a reasonable timeframe upon reasonable request. Raw neurophysiological datasets will also be made available to the scientific community upon reasonable request via the *RUcore* at Rutgers University (rucore.libraries.rutgers.edu/research/).

Statistical Analysis – Behavioral Responses. Days to reach the 80% performance criterion was compared between groups using Wilcoxon rank-sum tests, and the proportion of rapid learners (≥80% criterion reached within 10 days) was evaluated using Fisher's Exact tests. Behavioral responses during the Memory Test were analyzed using Linear Mixed-Effects Models with fixed effects of Frequency, Group, and their interaction, with planned contrasts assessing frequency-specific biases. Behavioral engagement across noise conditions was analyzed using mixed-design ANOVA.

Statistical Analysis – AC Responses. Electrophysiological responses to tones were analyzed using Linear Mixed-Effects Models conducted separately for each SNR condition, with fixed effects of Frequency and Group (TRAINED, TRAINED+RGFP966, NAÏVE) and their interaction. Post-hoc comparisons were corrected using Tukey or Bonferroni procedures. Steady-state noise-evoked activity, extracted from the pre-tone noise window, was analyzed using one-way ANOVA with Group as the independent factor, followed by Bonferroni-corrected pairwise tests where appropriate. All comparisons used two-tailed tests unless otherwise noted when motivated by *a priori* hypothesis of directional effects between groups or frequency factors. Alpha levels were $\alpha = 0.05$. Statistical analyses were conducted using MATLAB© (v2021b), R Statistical Software (v4.4.0), and JASP (v0.18.3).

RESULTS

Auditory learning is accelerated with post-training HDAC3 inhibition

Performance on the tone-reward associative task was evaluated across the full training cohort (n = 25). All rats successfully learned to bar-press to the tone cue for reward and ultimately reached high levels of asymptotic performance (**Fig. 1A**). As shown in Figure 1A, RGFP966-treated rats (n = 10/25) displayed earlier and steeper acquisition trajectories than identically trained but untreated controls (n = 15/25), with group means diverging primarily during the early training days. RGFP966-treated rats reached the 80% performance criterion faster than untreated rats (9.75 vs. 11.8 days; **Fig. 1B, C**). Therefore, a 10-day threshold was used to define rapid learners, i.e., as animals reaching criterion in fewer than 10 training days. In the full cohort, 7 of 10 RGFP966-treated rats and only 5 of 15 untreated rats met this threshold. Although this difference in proportions was not statistically significant ($p = 0.11$, odds ratio = 0.21, one-tailed Fisher's Exact test; **Fig. 1D**), the cumulative distribution of criterion attainment displayed a visually clear leftward shift in the RGFP966 group, consistent with an effect of HDAC3 inhibition to accelerate learning (**Fig. 1C**). Further neural analyses were limited to animals with successful electrophysiological cortical mapping that made data available across the targeted frequency representations in primary auditory cortex (see *Methods*; n = 13/25). Within this mapped subset, more RGFP966-treated rats (6 out of 7) than untreated rats (1 out of 6) reached criterion within 10 days ($p = 0.025$, odds ratio = 0.03, one-tailed Fisher's Exact test), mirroring the observed effect of HDAC3 inhibition across the full training cohort to accelerate learning. To avoid performance-related confounds that could introduce variability in analyses to identify the neural substrates of HDAC3-inhibition, the slowest-learning RGFP966-treated animal and the fastest-learning untreated animal were both excluded as outliers. Following these exclusions, neurophysiological analyses on AC frequency coding were conducted on a trained sub-group treated with the HDAC3-inhibitor (TRAINED+RGFP966; n = 6) and compared to the identically trained, but untreated group (TRAINED; n = 5). By definition, these groups differed in rate of task acquisition. RGFP966-treated rats were faster to learn the tone-reward association (Wilcoxon rank-sum test: $W < 0.001$, $p = 0.007$; **Fig. 1E, F**).

HDAC3 inhibition during training facilitates frequency-specific auditory cortical activity under low noise conditions

Frequency response areas (FRAs) were determined for each auditory cortical recording site in both trained groups and also in an untrained group of rats (NAÏVE; n = 7) to evaluate the effect of background noise on tone-evoked activity related to task learning. A region of interest within each FRA was defined as three test frequencies targeting the training tone frequency (i.e., 5.0kHz) and novel tones nearby (4.2kHz and 5.9kHz) either at the training tone sound level (i.e., 60 dB SPL) or at a lower sound level (40 dB SPL) for analysis in the three SNR conditions (**Fig. 2**). Spike rates were normalized (Z-scored sp/s) across recording sites to facilitate group-level analyses per SNR condition (SNR∞, SNR40, SNR20).

In quiet (SNR∞), the 5.9 kHz tone elicited the strongest relative evoked activity in all groups (60 dBs, Frequency: $F(2,771) = 8.86$, $p = 0.00016$; Group: $F(2,771) < 0.001$, $p = 1.00$; Frequency x Group: $F(4,771) = 2.24$, $p = 0.062$). Responses to 5.9 kHz were significantly higher than responses to 4.2 kHz (post hoc Linear Mixed-Effects Model contrasts collapsed across groups (Tukey-corrected) estimate = -0.298, $t(514) = -4.16$, $p = 0.0001$) and higher than responses to 5.0 kHz (estimate = -0.19, $t(514) = -2.65$, $p = 0.022$; **Fig. 3A**). The AC response bias to 5.9 kHz was not evident when presented at sound levels below the 60 dB training sound level, e.g., at 40 dBs (40 dBs, Frequency: $F(2, 771) = 0.14$, $p = 0.86$). Similarly, just as there was no significant effect of training or of the HDAC3-inhibitor at the training tone sound level, there were no significant effects at the lower sound level (40dBs, Group: $F(2, 771) < 0.001$ $p = 1.00$; Group x Frequency: $F(4, 771) = 0.24$ $p = 0.91$; **Fig. 3B)**.

The effect of adding a novel background of low noise (SNR40) was investigated to contrast with tone-evoked activity in quiet conditions (SNR∞). Interestingly, a learning-induced effect on AC response bias emerged that was frequency selective under low levels of background noise in animals treated with the HDAC3 inhibitor during auditory learning (60 dB: Group: $F(2, 771) < 0.001$, $p = 1.00$; Frequency: $F(2, 771) = 4.15$, $p = 0.016$; Frequency x Group: $F(4, 771) = 6.55$, $p < 0.001$; Linear Mixed-Effects Model, **Fig. 3C**). Within TRAINED+RGFP966-treated rats, spike rates evoked by 5.9 kHz were higher compared to activity evoked both by 5.0 kHz and 4.2 kHz (Tukey corrected t-tests for TRAINED+RGFP966: 5.0 kHz vs. 5.9 kHz: estimate = -0.521, $t(514) = -4.57$, $p < 0.0001$; 4.2 kHz vs. 5.9 kHz: estimate = -0.516, $t(514) = -4.53$, $p < 0.0001$), which were also higher than tone-evoked activity to 5.9 kHz in the untreated TRAINED group (Tukey corrected t-test: estimate = 0.504, $t(771) = 3.97$, $p = 0.0002$; **Fig. 3C**). Group differences in low background noise were abolished at lower sound levels of tone presentation (40 dB, Group: $F(2, 771) < 0.001$, $p = 1.00$; Frequency x Group: $F(4, 771) = 0.81$, $p = 0.51$; Mixed-Effects Model; **Fig. 3D**), though responding continued to be strongest to the 5.9 kHz tone (Frequency: $F(2,771) = 4.75$, $p = 0.008$; Tukey corrected posthoc: 5.0 kHz vs. 5.9 kHz: estimate = -0.215, $t(514) = -2.97$, $p = 0.008$; 4.2 kHz vs. 5.9 kHz: estimate = -0.159, $t(514) = -2.19$, $p = 0.073$; **Fig. 3D**).

Strikingly, auditory cortical frequency selectivity in the TRAINED+RGFP966 group under low level background noise conditions was abolished in conditions of the highest levels of background noise (SNR20). Although there was a trend towards the same AC response bias to 5.9 kHz (60 dB, Frequency: $F(2,771) = 3.26$, $p = 0.38$; Tukey-corrected posthoc test: 4.2 kHz vs 5.9 kHz: estimate = -0.176, $t(514) = -2.42$, $p = 0.04$; 5.0 kHz vs 5.9 kHz: estimate = -0.138, $t(514) = -1.902$,

p = 0.14; 4.2 kHz vs. 5.0 kHz: estimate = -0.038, t(514) = -0.52, p = 0.85), it did not depend on RGFP966 treatment or training (Group: F(2, 771) < 0.001, p = 1.00; Frequency x Group: F(4, 771) = 0.99, p = 0.41; Linear Mixed-Effects Model; **Fig. 3E**). At lower sound levels of tone presentations in high noise, any evidence of group or frequency effects were eradicated (40 dBs, Frequency: F(2, 771) = 0.69, p = 0.49; Group: F(2, 771) < 0.001, p = 1.00; Frequency x Group: F(4, 771) = 1.93, p = 0.10; Linear Mixed-Effects Model; **Fig. 3F**). Altogether, the data support that tone-reward learning induces a frequency-selective preservation of an auditory cortical response bias that can survive in low noise conditions and may be amplified under conditions of rapid task acquisition promoted by RGFP966 treatment.

Auditory cortical responses to steady-state noise are suppressed in animals treated with an HDAC3 inhibitor during auditory learning

To explore the possibility that learning-induced effects mediated by RGFP966 could have effects on auditory cortical responses during steady-state noise alone, evoked activity during the time period *immediately prior* to tone onset was analyzed. Data are plotted across trials binned by the forthcoming tone frequency to-be-played on that trial for visualization. Overall, there was a suppression of auditory cortical responses to steady-state noise in trained animals when presented with 0 dB noise (Group: F(2,257) = 5.04, p = 0.007; **Fig. 4A**), with 20 dB noise (Group: F(2,257) = 5.18, p = 0.006; **Fig. 4B**), and with 40dB noise (Group: F(2,257) = 10.16, p < 0.001; **Fig. 4C**) that was most pronounced in TRAINED+RGFP966-treated animals (0 dB noise, Bonferroni corrected posthoc: TRAINED+RGFP966 vs. NAÏVE: t(191) = -3.17, p = 0.005; TRAINED+RGFP966 vs. TRAINED: t(164) = -1.35, p = 0.532; TRAINED vs. NAÏVE: t(159) = 1.52, p = 0.388; 20 dB noise, Bonferroni corrected posthoc: TRAINED+RGFP966 vs. NAÏVE: t(191) = -3.17, p = 0.005; TRAINED+RGFP966 vs. TRAINED: t(164) = -1.35, p = 1.00; TRAINED vs. NAÏVE: t(159) = 1.52, p = 0.151; 40 dB noise, Bonferroni corrected posthoc: TRAINED+RGFP966 vs. NAÏVE: t(191) = -4.50, p < 0.001; TRAINED+RGFP966 vs. TRAINED: t(164) = -2.11, p = 0.107; TRAINED vs. NAÏVE: t(159) = 1.97, p = 0.150). Together, these data suggest that a general outcome of auditory learning is to suppress auditory cortical responses to steady-state noise that can be strengthened under conditions of rapid task acquisition with RGFP966 treatment.

Spontaneous auditory cortical activity during quiet inter-stimulus intervales is not affected by training or treatment with an HDAC3 inhibitor

To investigate whether the suppressive effect on sound-evoked activity in trained and RGFP966-treated animals could be explained by an overall suppression of auditory cortical excitability, spontaneous auditory cortical activity during silent inter-trial intervals was analyzed. Spontaneous rate was not different between groups (F(2, 257) = 1.27, p = 0.282, **Fig. 4D**). This finding bolsters the finding that lower cortical activity identified during periods of steady-state noise after training and RGFP966 treatment is most likely the result of a suppressive effect on noise-evoked auditory cortical activity *per se*.

Background noise decreases behavioral task engagement

To evaluate how background noise may have had a general impact on behavioral engagement in the tone-reward task, a behavioral memory test was conducted to present tones under different SNRs that paralleled the background noise conditions used for electrophysiological recordings

during auditory cortical mapping (see *Methods*). Bar-press responses to tones in both groups progressively decreased in graded steps between quiet and higher noise conditions (Noise: $F(4, 36) = 48.99$, $p < 0.001$; Group: $F(1, 9) = 0.13$, $p = 0.72$; Noise x Group: $F(4, 36) = 0.41$, $p = 0.80$, Mixed-ANOVA; **Fig. 5**). Interestingly, the number of bar-presses that occurred in the highest noise condition (60 dB noise, SNR0) did not differ from the number of bar-presses made during trials of only white noise (i.e. 60 dB Gaussian noise) that did not include the presentation of a concurrent tone (Bonferroni corrected t-test: $t(9) = -1.30$, $p = 1.00$); both produced near-zero responding in the TRAINED+RGFP966 and TRAINED groups. Because white noise and high noise (SNR0) conditions were statistically indistinguishable and yielded insufficient behavioral variance to estimate frequency selectivity, these conditions are reported descriptively but were excluded from mixed-effects analyses of frequency-selective memory in the next set of analyses.

The behavioral expression of frequency-specific memory recapitulates auditory cortical responses

A surprising finding in the auditory cortical datasets was the discovery that the 5.9 kHz test tone frequency evoked the highest rate of auditory cortical responding, including in low backgrounds of noise. To determine whether the selectivity of the cortical response to 5.9 kHz had an impact on behavioral response selectivity, the behavioral memory test conducted in the same animals was analyzed to determine the likelihood of responding to one of three different frequencies after achieving high levels of asymptotic performance. Given that the overall behavioral engagement was equivalent between treatment groups (as shown in **Fig. 5)**, it was reasonable to use this analysis to approximate the effects of noise on frequency-selective tone detection in behavior. Memory testing included the training tone (5.0 kHz) and two nearby novel test frequencies (4.2 kHz and 5.9 kHz). Both TRAINED+RGFP966 and TRAINED groups displayed a frequency-selective behavioral response bias revealed by higher responding to the 5.9 kHz cue in quiet (SNR∞; Frequency: $F(2,24) = 10.89$, $p = 0.0004$; Treatment: $F(1,24) < 0.001$, $p = 1.00$; Group × Frequency: $F(2,24) = 2.13$, $p = 0.14$; Linear Mixed-Effects, **Fig. 6A**). Frequency-selectivity for responding more to 5.9 kHz than to the other two tone frequencies was pronounced (planned contrasts averaged across groups: 5.9 kHz vs. 5.0 kHz, $t(16) = 4.60$, $p = 0.0003$; 5.9 kHz vs. the mean of 4.2 and 5.0 kHz, $t(16) = 4.37$, $p = 0.0005$). Interestingly, the addition of low-level background noise (20 dB noise; SNR40) paradoxically elevated the behavioral expression of frequency selectivity. Both groups showed markedly elevated responding to the 5.9 kHz test tone in both groups (Frequency: $F(2, 24) = 15.20$, $p < 0.0001$; Group: $F(1, 24) < 0.0001$, $p = 1.00$; Group × Frequency: $F(2, 24) = 0.17$, $p = 0.85$, Mixed-Effects Model; planned contrast comparing 5.9 kHz to the mean of 4.2 and 5.0 kHz, $t(16) = 5.48$, $p = 0.0001$; **Fig. 6B**). In contrast, higher noise backgrounds (40 dB noise; SNR20) disrupted the expression of signal-specific memory toward the 5.9-kHz cue. Neither tone frequency nor treatment significantly influenced responding (Frequency: $F(2,24) = 1.85$, $p = 0.18$; Group: $F(1, 24) < 0.001$, $p = 1.00$; Group × Freq: $F(2, 24) = 0.09$, $p = 0.92$; **Fig. 6C**). In line with the prior reported finding of poor behavioral engagement during high noise conditions, frequency-selective contrasts collapsed across groups did not reach significance ($t(16) = 1.68$, $p = 0.11$), indicating that the highest noise tested condition completed abolished the expression of behavioral response selectivity for tone frequency that had emerged under low noise conditions. The behavioral response bias to the 5.9 kHz tone is a remarkable match to the auditory cortical tone-evoked response patterns. This match is even more

remarkable when considering that the sound frequency presented during tone-reward task training was 5.0 kHz, while the behavioral and neural response bias were both peak-shifted to the 5.9 kHz frequency. Even more remarkable was the match observed in auditory cortical and behavioral nonlinearity to enhance and then abolish frequency-selective response biases with increasing background noise conditions from low to high, respectively.

DISCUSSION

The present study identifies a set of learning-dependent mechanisms that shape how auditory cortex encodes behaviorally relevant signals that are revealed in the presence of background noise. Across behavioral and electrophysiological measures, background noise degraded expression of a learned sound-specific memory, consistent with extensive human literature showing that speech and word recognition deteriorate as noise levels increase despite constant SNR (e.g., Pollack and Pickett, 1958; Dubno et al., 2005). The findings show that associative learning reorganizes the representation of frequency-specific cortical responses in ways that remain detectable and even amplified under modest acoustic interference. Pharmacological inhibition of HDAC3 strengthens this representational plasticity by selectively enhancing AC activity evoked by the learned signal while suppressing noise-driven responsivity. Together, the results reveal a coordinated pattern of neural plasticity in which associative learning and HDAC3-regulated neuroplasticity interact to improve signal processing in the auditory cortex and behavior under degraded acoustic conditions. These findings extend classical views of auditory cortical plasticity by demonstrating that the expression of learned representations is not fixed, but instead emerges through dynamic interactions between cortical effects of prior learning outcomes and ongoing acoustic context (Brandon et al., 2003). More broadly, our results position HDAC3-regulated neuroplasticity as a key molecular process that may determine when and under what sensory conditions cortical plasticity can support sound-guided behavior relevant to listening comprehension.

A central result is that frequency-selective AC response biases were latent in quiet conditions and became robustly expressed under low levels of background noise, and even more so in RGFP966-treated learners. This demonstrates that noise can serve as a probe for latent learning-dependent tuning changes, akin to latent learning frameworks proposed in other systems (Lubow and Moore, 1959; Kuchibhotla et al., 2019; Drieu et al., 2025). Under low noise (SNR40), the learned response bias toward 5.9 kHz becomes amplified, whereas under higher noise (SNR20) this selectivity collapses entirely. This nonlinear pattern suggests that background noise interacts with the stability of learned cortical representations, revealing a threshold beyond which noise disrupts the latent expression of plasticity-driven memory traces. These findings support a mechanistic model in which learning-induced frequency-selective auditory cortical plasticity confers robustness only within a constrained dynamic noise range, beyond which cortical suppression mechanisms dominate and mask frequency-selective coding. This dynamic conditionality highlights that learned auditory memories are not expressed uniformly across contexts, but rather depend on the interplay between representational strength and sensory interference. Further, an interaction between noise-driven and RGFP966-driven changes in AC coding reveals an intriguing mechanistic convergence. Prior work showed that background noise

can paradoxically improve discrimination between adjacent frequencies by reducing receptive field overlap among neighboring channels (Christensen et al., 2019). HDAC3 inhibition can produce a similar reduction in neural overlap by narrowing signal-specific tuning bandwidth (Bieszczad et al., 2015; Shang et al., 2019; Rotondo and Bieszczad, 2020, 2021a). In the present study, HDAC3 inhibition preserved noise-induced frequency selectivity for the target sound. Together, these results suggest that HDAC3-mediated regulation of auditory cortical plasticity supports the stability of key coding features like frequency tuning selectivity and increased sound-evoked responses that are likely required for accurate signal-in-noise detection.

A second major finding is that HDAC3 inhibition selectively suppresses steady-state noise responses without altering spontaneous cortical activity. This indicates that HDAC3-dependent plasticity enhances cortical signal-to-noise ratios not by increasing excitability broadly, but by shaping how the auditory cortex responds to noise. Across several noise levels, RGFP966-treated animals displayed markedly reduced noise-evoked firing relative to naïve animals and relative to untreated, less rapid learners, even though the noise challenge had not been present during task acquisition. The absence of differences in spontaneous firing is consistent with prior reports against global hyperexcitability as a mechanism of signal-in-noise detection (Christensen et al., 2025). Instead, the data point to a shift in the balance between excitatory and inhibitory processing that enhances relative responsivity to the remembered signal by suppressing responses to non-informative background noise (Teschner et al., 2016; Christensen et al., 2019; Lakunina et al., 2022; Mischler et al., 2023). This mechanism is metabolically conservative: rather than increasing overall activity, HDAC3 inhibition redistributes cortical responsivity in a way that prioritizes behaviorally relevant information while minimizing the energetic cost of background noise processing. An intriguing implication of this finding relates to the “chicken-and-egg” question of whether rapid-learning animals possessed *a priori* cortical properties like reduced responsivity to noise that facilitated faster task acquisition. While RGFP966 treatment correlated with the accelerated learning reported across the large cohort of rats trained in this study, the possibility nonetheless remains that animals naturally predisposed to low noise-driven cortical excitability may be more efficient learners because they experience an inherently improved neural signal-to-noise ratio during task learning. More broadly, this raises an empirical hypothesis that mitigating noise during learning using biological or environmental manipulations could facilitate learning and memory outcomes. This hypothesis has support in broadly relevant educational and clinical settings (Bronzaft, 1981; Alain et al., 2014; Kuchinsky et al., 2016; Krizman et al., 2017; Hennessy et al., 2021), suggesting that reducing acoustic interference may disproportionately benefit individuals with inherently weaker cortical suppression mechanisms.

The enhanced expression of frequency-selective biases specifically under low noise in RGFP966-treated animals highlights that HDAC3-regulated neuroplasticity supports the stabilization of high-fidelity representations that remain decodable under moderately degraded conditions. However, HDAC3 inhibition does not make cortical processing noise-proof. At higher levels of acoustic interference, frequency selectivity was abolished in treated and untreated animals alike, indicating that HDAC3-regulated plasticity extends, but does not remove the operational limits under which learned auditory representations can be expressed. This distinction is mechanistically important: HDAC3 inhibition increases representational robustness but does not override the physiological

constraints imposed by strong sensory noise. For example, stream segregation depends critically on prior knowledge, and memory for a sound can enhance its segregation from background noise (Bregman, 1994; Snyder and Alain, 2007). The present study demonstrates distinct cortical responses in noise compared to quiet, that are usually selectively vulnerable to degradation by noise. Learning processes can rescue a sound signal's vulnerability to noise, and by enhancing the stability of memory traces, HDAC3 inhibition may promote a more distinct separation between neural populations responding to a learned signal sound relative to those responding to novel sounds and to background noise. This echoes prior observations that sparse neural populations in primary and secondary auditory cortices can encode behaviorally relevant sounds in a noise-invariant manner to some limit (Schneider and Woolley, 2013; Kang and Kanold, 2023). The present study adds to this literature to go beyond important studies conducted under passive exposure without behavioral correlates, to now link learning experience and behavioral outcomes to AC physiology, and the behavioral outcomes of learning-dependent plasticity on signal responsivity in noisy contexts.

A consistent and striking observation across neural and behavioral datasets was the peak-shifted responsivity bias toward the 5.9 kHz test frequency rather than the 5.0 kHz training frequency. This shift represents a mechanistic signature of associative generalization and receptive field reweighting, consistent with classical behavioral findings (e.g., the "peak shift" phenomenon; Purtle, 1973) and with studies showing receptive field changes centered around behaviorally salient rather than veridically trained features (Miasnikov and Weinberger, 2012). The enhanced responses to 5.9 kHz observed both cortically and behaviorally underscore the idea that auditory learning modifies population coding in a way that emphasizes the most discriminable or behaviorally-reinforced spectral representations. This pattern aligns with evidence that learning engages transient neural states during encoding that shapes later behavior independently of stimulus accuracy. For example, prior work has shown that stimulus-induced gamma-band activity during learning predicts subsequent behavioral responding not only for reinforced tone signals, but also for explicitly non-reinforced tone signals in a way that depends on the degree of gamma induced to drive tone-selective cortical plasticity indicating that gamma-related cortical encoding processes can support internally generated and false memory-like representations rather than veridical stimulus-outcome associations (Gonsalves and Paller, 2000; Headley and Weinberger, 2011). Critically, gamma oscillations in this framework do not appear to maintain memories over time, but instead reflect a time-limited encoding mechanism that shapes how sensory information is integrated and later expressed (Headley and Weinberger, 2013). Within this framework, peak shift may emerge as a consequence of encoding states that bias cortical representations toward inferred or expected stimulus features rather than exact acoustic identity (Salinas and Sejnowski, 2000; Miasnikov and Weinberger, 2012). HDAC3-regulated plasticity may stabilize the impact of these encoding-related neural states that generate gamma, and extend the conditions under which learned representations can be robustly expressed in noise. Notably in the present findings, noise could amplify or suppress this peak shift depending on SNR, demonstrating that expression of the induced coding changes remains context-dependent, and that sensory interference can likewise modulate learned internal memory representations. A convergence of electrophysiological and behavioral data that does not depend on veridical features of stimuli in

the real world represents a rare and compelling example of parallel plasticity across levels of analysis that support causal brain-behavior relationships.

HDAC3 inhibition emerges from this work as a mechanistic probe for dissecting the cortical computations underlying listening in noise. By selectively enhancing the consolidation of frequency-specific learning without a global increase in cortical excitability, the specific neural features and circuit dynamics sufficient for accurate signal detection under challenging acoustic conditions could be investigated. The effects of RGFP966 revealed candidate features of auditory cortical coding that may be key for memory expression in noise. As such, the findings support that HDAC3 may be a molecular gatekeeper that regulates both the speed at which learning influences the cortical computations that support signal-in-noise detection and the stability with which those changes manifest under increasing sensory interference. Future work is needed to determine whether HDAC3-dependent preservation of AC coding predicts sound-specific behavior in noise within individual subjects. Further, noise challenges may interact differently with orthogonal temporal coding features that contribute to sound-specific memory CIT, suggesting the value of future tasks and analyses based on temporal precision and phase-locking, particularly for learning about temporally-rich acoustic cues. Finally, extending this work to aged animals could address whether HDAC3-mediated robustness in AC coding are possible in the aged brain, and if so, whether they can mitigate well-documented age-related declines in listening skills (Kuchinsky et al., 2016; Burns and Gräff, 2021; Shilling-Scrivo et al., 2021).

Overall, our findings support an integrated mechanistic model of how auditory learning shapes cortical processing to support listening in noise. Learning produces frequency-specific cortical plasticity that enhances signal detection under modest background noise while engaging complementary processes that suppress steady-state noise. HDAC3 inhibition appears to strengthen learning-induced processes and extends the noise range over which memory can be expressed. An interaction between environmental noise and representational strength defines the effective operational limits of auditory memory-guided listening. By linking epigenetic mechanisms to cortical coding dynamics and sound-guided behavior, this study broadens our understanding of how cortical plasticity is stabilized and deployed across sensory contexts. Molecular constraints on learning and memory consolidation may influence not only the persistence of auditory memories (Campbell and Wood, 2019; Shang and Bieszczad, 2022) but also their expression in real-world listening environments.

FIGURE LEGENDS

Figure 1. *Auditory learning is accelerated by post-training HDAC3 inhibition.* **(A)** Acquisition of tone–reward associative learning plotted as daily performance (% correct) across training days for the full cohort (n = 25). Thin lines represent individual animals; thick lines indicate group means (±SEM). Rats treated with the HDAC3 inhibitor RGFP966 (TRAINED+RGFP966; n = 10) exhibited earlier and steeper learning trajectories compared with identically trained but untreated controls (TRAINED; n = 15), with divergence most evident during early training. Dashed vertical lines indicate the mean day at which each group reached the 80% performance criterion. **(B)** Days required to reach the 80% performance criterion for RGFP966-treated and untreated rats in the full cohort. Individual animals are shown with group means ± SD overlaid; n.s., not significant. **(C)** Cumulative percentage of animals reaching the 80% criterion as a function of training day, demonstrating a leftward shift in the RGFP966-treated group indicative of accelerated learning. **(D)** Proportion of rapid learners, defined as animals reaching criterion in fewer than 10 training days, in the full cohort. Numbers within pie charts indicate animals reaching criterion in ≤10 days versus >10 days. **(E)** Acquisition curves for the subset of animals with successful auditory cortical mapping used for subsequent neurophysiological analyses (TRAINED+RGFP966, n = 6; TRAINED, n = 5), plotted as in A. Shaded region denotes the period used to assess acquisition rate, and dashed lines indicate mean criterion day for each group. **(F)** Days to reach the 80% criterion for the mapped subset shown in E. RGFP966-treated rats learned significantly faster than untreated rats (Wilcoxon rank-sum test; **$p < 0.01$).

Figure 2. *Definition of frequency response area (FRA) region of interest and effects of background noise on tone-evoked auditory cortical activity.* **(A)** Schematic of the electrophysiological trial structure used to assess tone-evoked responses in auditory cortex. A 25-ms pure tone was presented on each trial, embedded in either quiet (SNR∞) or background noise (SNR20 or SNR40). Tone onset was temporally jittered between 275 and 415 ms (20-ms increments) relative to trial start to reduce anticipatory responses. Background noise preceded and followed tone presentation, yielding fixed pre- and post-tone noise epochs for response estimation. **(B)** Example frequency response areas (FRAs) from a representative auditory cortical recording site obtained under quiet (SNR∞), low-noise (SNR40), and high-noise (SNR20) conditions. Color maps depict tone-evoked firing rate (spikes/s) as a function of tone frequency and sound level (dB SPL). The black boxed region indicates the predefined region of interest (ROI) used for quantitative analyses at 60 dB SPL tones. **(C)** Corresponding spike rasters (top row) and peristimulus time histograms (PSTHs; bottom row) for responses to 60-dB SPL tones presented at the training frequency within each SNR condition. Dashed vertical lines indicate tone onset.

Figure 3. *Learning- and noise-dependent modulation of auditory cortical frequency selectivity within the FRA region of interest.* Frequency response areas (FRAs) were quantified for auditory cortical recording sites in trained rats (TRAINED and TRAINED+RGFP966) and in an untrained control group (NAÏVE; n = 7). Analyses were restricted to a predefined FRA region of interest (ROI; Fig. 2) comprising three test frequencies centered on the training tone (5.0 kHz) and

adjacent novel frequencies (4.2 and 5.9 kHz), evaluated at the training sound level (60 dB SPL) and a lower sound level (40 dB SPL) across three background noise conditions (SNR∞, SNR40, SNR20). Spike rates were Z-scored across recording sites to normalize for between-site variability and enable group-level comparisons. Lines and shaded regions indicate group means SEM. **(A,B)** *Quiet (SNR∞).* At the training sound level (60 dB SPL; A), tone-evoked activity was frequency dependent across all groups, with the strongest responses observed at 5.9 kHz, independent of training or HDAC3 inhibition. At the lower sound level (40 dB SPL; B), frequency selectivity was abolished, and no effects of Group or Group × Frequency interactions were observed. **(C,D)** *Low background noise (SNR40).* Under low noise conditions at 60 dB SPL (C), a frequency-selective learning effect emerged that depended on HDAC3 inhibition. TRAINED+RGFP966 rats exhibited enhanced responses to the novel 5.9 kHz tone relative to both the training frequency (5.0 kHz) and the lower novel frequency (4.2 kHz), as well as relative to the untreated TRAINED group, reflected in a significant Frequency × Group interaction. This group-specific frequency selectivity was eliminated when tones were presented at 40 dB SPL (D), although responses remained strongest to 5.9 kHz across groups. **(E,F)** High background noise (SNR20). At the training sound level (60 dB SPL; E), frequency-dependent responding was weakened, and no effects of training or HDAC3 inhibition were detected despite a residual trend toward higher responses at 5.9 kHz. At the lower sound level (40 dB SPL; F), both frequency selectivity and group differences were fully abolished.

Figure 4. *Auditory cortical responses to steady-state noise are suppressed by auditory learning and are enhanced by HDAC3 inhibition, without changes in spontaneous activity.* Auditory cortical firing rates during steady-state background noise were quantified in trained rats (TRAINED and TRAINED+RGFP966) and untrained controls (NAÏVE). Analyses focused on the pre-tone epoch immediately preceding tone onset, isolating noise-evoked activity independent of tone-evoked responses. For visualization, data are plotted as a function of the forthcoming tone frequency on each trial. Lines and shaded regions denote group means ± SEM. **(A–C)** Steady-state noise-evoked activity. Mean firing rates during steady-state noise preceding tone presentation are shown for three noise levels: 0 dB noise prior to a 40 dB tone (A), 20 dB noise prior to a 60 dB tone (B), and 40 dB noise prior to a 60 dB tone (C). Across all three noise conditions, auditory cortical responses to steady-state noise were significantly reduced in trained animals, with the strongest suppression observed in TRAINED+RGFP966-treated rats. Group effects were present at all noise levels and were driven primarily by reduced activity in the TRAINED+RGFP966 group relative to NAÏVE animals, while differences between TRAINED and NAÏVE rats did not reach significance. Suppression of noise-evoked activity was progressively more pronounced as background noise level increased. **(D)** Spontaneous activity in quiet. True spontaneous firing rates measured during silent inter-trial intervals in quiet conditions did not differ between NAÏVE, TRAINED, and TRAINED+RGFP966 groups, indicating that training- and RGFP966-related reductions in activity are specific to sound-evoked responses during steady-state noise and do not reflect a global suppression of auditory cortical excitability.

Figure 5. *Background noise produces a graded reduction in behavioral responding during the tone-reward memory test, independent of HDAC3 inhibition.* Rats previously trained on the tone-reward task (TRAINED and TRAINED+RGFP966) were tested with tone presentations embedded

in progressively higher levels of background noise that paralleled the signal-to-noise ratio (SNR) conditions used during auditory cortical mapping (see *Methods*). Bars show group means ± SEM, with thin lines indicating individual animals. Because white noise and high-noise (SNR0) conditions were statistically indistinguishable and yielded minimal behavioral variance, they are shown for completeness but were excluded from subsequent mixed-effects analyses of frequency-selective memory performance.

Figure 6. *Behavioral expression of frequency-specific memory mirrors auditory cortical response selectivity and its modulation by background noise.* Memory tests were conducted in the same animals used for physiological analyses and included the training frequency (5.0 kHz) and two nearby novel frequencies (4.2 and 5.9 kHz). Proportion of bar-press responses is shown for TRAINED and TRAINED+RGFP966 groups; thin lines indicate individual animals, and thick lines denote group means. **(A)** *Quiet (SNR∞).* In the absence of background noise, both groups exhibited a frequency-selective behavioral response bias, with significantly higher responding to the 5.9 kHz tone compared with the training frequency (5.0 kHz) and the mean of training frequency and lower novel frequency (4.2 kHz). This effect was independent of RGFP966 treatment, as evidenced by a significant main effect of Frequency without Group or Group × Frequency interactions. **(B)** *Low background noise (SNR40; 20 dB noise).* The addition of low-level background noise paradoxically enhanced the behavioral expression of frequency selectivity. Both TRAINED and TRAINED+RGFP966 animals showed markedly elevated responding to the 5.9 kHz tone relative to the other frequencies, yielding a stronger main effect of Frequency while remaining independent of treatment group. **(C)** *Higher background noise (SNR20; 40 dB noise).* In contrast, higher levels of background noise abolished frequency-selective responding.

SUPPLEMENTARY FIGURE LEGENDS

Figure S1. *Vehicle injections do not alter acquisition of the tone-reward task.* **(A)** Acquisition curves showing daily performance across training days for vehicle-injected and non-injected trained animals. Thin lines represent individual animals, and thick lines indicate group means ± SEM. Dashed vertical lines denote the mean day at which each group reached the 80% performance criterion. Both groups exhibited similar learning trajectories and reached asymptotic performance over comparable time courses. **(B)** Days required to reach the 80% performance criterion for vehicle-injected and non-injected animals. Individual animals are shown with group means ± SEM overlaid; no significant difference was observed between groups. **(C)** Cumulative percentage of animals reaching the 80% criterion as a function of training day, illustrating overlapping acquisition dynamics for vehicle-injected and non-injected animals. The mean number of days to reach criterion did not differ between vehicle-injected and non-injected rats (Wilcoxon rank-sum test, $p = 0.72$).

Figure S2. *Experimental timeline for learning the tone-reward task, memory testing, and auditory cortical electrophysiological recording.* **(A)** *Experimental timeline.* Animals underwent bar-press shaping followed by tone-reward training in Quiet. Post-session injections of the selective HDAC3 inhibitor RGFP966 or vehicle treatment were administered immediately after training sessions on days 2, 3 and 4. Training in quiet conditions continued daily until animals reached the acquisition criterion. Upon attaining criterion, animals completed a behavioral memory test in a novel background of different noise conditions, followed 24-48 hrs later by a final reinforced training session in Quiet to confirm stable task performance prior to auditory cortical electrophysiological recordings. **(B)** *Tone-reward training in Quiet.* During training sessions, a single 5.0 kHz tone was presented in quiet. Bar presses occurring during tone presentation were reinforced with water reward, whereas responses outside the tone window were not reinforced. **(C)** *Memory test in Noise.* To ensure stable task engagement immediately prior to memory testing, animals completed a brief reinforced warm-up session (~5 min) that was immediately followed by the memory test. During the memory test, tones were presented without reinforcement, and bar-press responses were recorded as a measure of memory-guided behavior. **(D)** *Acoustic structure of memory test stimuli.* Memory test trials consisted of an 8-s tone presented either in quiet (SNR∞) or embedded in notched Gaussian white noise at three signal-to-noise ratios: low noise (60 dB tone + 20 dB noise; SNR40), medium noise (60 dB tone + 40 dB noise; SNR20), and high noise (60 dB tone + 60 dB noise; SNR0).

Figure S3. *Memory testing does not disrupt subsequent tone–reward task performance.* All animals completed an additional tone-reward training session 24-48 hrs after memory testing. **(A)** *Within-animal performance stability.* Performance during the final reinforced training trial conducted before memory testing was compared with performance during the reinforced session conducted after memory testing. Individual animals are shown with paired data points connected by lines; bars represent group means ± SEM. Performance levels did not differ between pre- and post-memory test sessions, indicating that memory test did not disrupt task performance. **(B)** *Between-group comparison after memory testing.* Performance during the post-memory test training session is shown separately for TRAINED and TRAINED+RGFP966 animals. Individual animals are overlaid on violin plots depicting the distribution of performance values, with group

means ± SEM indicated. Final performance did not differ between groups, demonstrating equivalent task proficiency following memory testing.

REFERENCES

Aizenberg M, Mwilambwe-Tshilobo L, Briguglio JJ, Natan RG, Geffen MN (2015) Bidirectional Regulation of Innate and Learned Behaviors That Rely on Frequency Discrimination by Cortical Inhibitory Neurons. PLOS Biol 13:e1002308.

Alain C, Zendel BR, Hutka S, Bidelman GM (2014) Turning down the noise: the benefit of musical training on the aging auditory brain. Hear Res 308:162–173.

Bieszczad KM, Bechay K, Rusche JR, Jacques V, Kudugunti S, Miao W, Weinberger NM, McGaugh JL, Wood MA (2015) Histone Deacetylase Inhibition via RGFP966 Releases the Brakes on Sensory Cortical Plasticity and the Specificity of Memory Formation. J Neurosci 35:13124–13132.

Bieszczad KM, Weinberger NM (2010) Representational gain in cortical area underlies increase of memory strength. Proc Natl Acad Sci U S A 107:3793–3798.

Blackwell JM, Geffen MN (2017) Progress and challenges for understanding the function of cortical microcircuits in auditory processing. Nat Commun 8:2165.

Brandon SE, Vogel EH, Wagner AR (2003) Stimulus representation in SOP: I. Theoretical rationalization and some implications. Behav Processes 62:5–25.

Bregman AS (1994) Auditory Scene Analysis: The Perceptual Organization of Sound. MIT Press.

Bronzaft AL (1981) The effect of a noise abatement program on reading ability. J Environ Psychol 1:215–222.

Burns AM, Gräff J (2021) Cognitive epigenetic priming: leveraging histone acetylation for memory amelioration. Curr Opin Neurobiol 67:75–84.

Campbell RR, Wood MA (2019) How the epigenome integrates information and reshapes the synapse. Nat Rev Neurosci 20:133–147.

Christensen RK, Lindén H, Nakamura M, Barkat TR (2019) White Noise Background Improves Tone Discrimination by Suppressing Cortical Tuning Curves. Cell Rep 29:2041-2053.e4.

Christensen RK, Studer F, Barkat TR (2025) Background white noise increases neuronal activity by reducing membrane fluctuations and slow-wave oscillations in auditory cortex. Prog Neurobiol 246:102720.

Drieu C, Zhu Z, Wang Z, Fuller K, Wang A, Elnozahy S, Kuchibhotla K (2025) Rapid emergence of latent knowledge in the sensory cortex drives learning. Nature 641:960–970.

Dubno JR, Horwitz AR, Ahlstrom JB (2005) Word recognition in noise at higher-than-normal levels: Decreases in scores and increases in masking. J Acoust Soc Am 118:914–922.

Fritz J, Shamma S, Elhilali M, Klein D (2003) Rapid task-related plasticity of spectrotemporal receptive fields in primary auditory cortex. Nat Neurosci 6:1216–1223.

Froemke RC (2015) Plasticity of Cortical Excitatory-Inhibitory Balance. Annu Rev Neurosci 38:195–219.

Gonsalves B, Paller KA (2000) Neural events that underlie remembering something that never happened. Nat Neurosci 3:1316–1321.

Graham G, Chimenti MS, Knudtson KL, Grenard DN, Co L, Sumner M, Tchou T, Bieszczad KM (2023) Learning induces unique transcriptional landscapes in the auditory cortex. bioRxiv:2023.04.15.536914.

Headley DB, Weinberger NM (2011) Gamma-band activation predicts both associative memory and cortical plasticity. J Neurosci Off J Soc Neurosci 31:12748–12758.

Headley DB, Weinberger NM (2013) Fear conditioning enhances γ oscillations and their entrainment of neurons representing the conditioned stimulus. J Neurosci Off J Soc Neurosci 33:5705–5717.

Hennessy S, Wood A, Wilcox R, Habibi A (2021) Neurophysiological improvements in speech-in-noise task after short-term choir training in older adults. Aging 13:9468–9495.

Kang H, Kanold PO (2023) Auditory memory of complex sounds in sparsely distributed, highly correlated neurons in the auditory cortex. bioRxiv:2023.02.02.526903.

Krizman J, Bradlow AR, Lam SS-Y, Kraus N (2017) How bilinguals listen in noise: linguistic and non-linguistic factors. Biling Lang Cogn 20:834–843.

Kuchibhotla KV, Hindmarsh Sten T, Papadoyannis ES, Elnozahy S, Fogelson KA, Kumar R, Boubenec Y, Holland PC, Ostojic S, Froemke RC (2019) Dissociating task acquisition from expression during learning reveals latent knowledge. Nat Commun 10:2151.

Kuchinsky SE, Vaden KI, Ahlstrom JB, Cute SL, Humes LE, Dubno JR, Eckert MA (2016) Task-Related Vigilance During Word Recognition in Noise for Older Adults with Hearing Loss. Exp Aging Res 42:50–66.

Lakunina AA, Menashe N, Jaramillo S (2022) Contributions of Distinct Auditory Cortical Inhibitory Neuron Types to the Detection of Sounds in Background Noise. eNeuro 9 Available at: https://www.eneuro.org/content/9/2/ENEURO.0264-21.2021 [Accessed December 14, 2025].

Lubow RE, Moore AU (1959) Latent inhibition: the effect of nonreinforced pre-exposure to the conditional stimulus. J Comp Physiol Psychol 52:415–419.

McGann JP (2015) Associative learning and sensory neuroplasticity: how does it happen and what is it good for? Learn Mem Cold Spring Harb N 22:567–576.

Miasnikov AA, Weinberger NM (2012) Detection of an inhibitory cortical gradient underlying peak shift in learning: a neural basis for a false memory. Neurobiol Learn Mem 98:368–379.

Mischler G, Keshishian M, Bickel S, Mehta AD, Mesgarani N (2023) Deep neural networks effectively model neural adaptation to changing background noise and suggest nonlinear noise filtering methods in auditory cortex. NeuroImage 266:119819.

Natan RG, Rao W, Geffen MN (2017) Cortical Interneurons Differentially Shape Frequency Tuning following Adaptation. Cell Rep 21:878–890.

Nocon JC, Gritton HJ, James NM, Mount RA, Qu Z, Han X, Sen K (2023) Parvalbumin neurons enhance temporal coding and reduce cortical noise in complex auditory scenes. Commun Biol 6:751.

Phan ML, Bieszczad KM (2016) Sensory Cortical Plasticity Participates in the Epigenetic Regulation of Robust Memory Formation. Neural Plast 2016:7254297.

Phillips DP (1985) Temporal response features of cat auditory cortex neurons contributing to sensitivity to tones delivered in the presence of continuous noise. Hear Res 19:253–268.

Phillips DP, Hall SE (1986) Spike-rate intensity functions of cat cortical neurons studied with combined tone-noise stimuli. J Acoust Soc Am 80:177–187.

Pollack I, Pickett JM (1958) Masking of Speech by Noise at High Sound Levels. J Acoust Soc Am 30:127–130.

Purtle RB (1973) Peak shift: A review. Psychol Bull 80:408–421.

Rotondo EK, Bieszczad KM (2020) Precise memory for pure tones is predicted by measures of learning-induced sensory system neurophysiological plasticity at cortical and subcortical levels. Learn Mem 27:328–339.

Rotondo EK, Bieszczad KM (2021a) Sensory cortical and subcortical auditory neurophysiological changes predict cue-specific extinction behavior enabled by the pharmacological inhibition of an epigenetic regulator during memory formation. Brain Res Bull 169:167–183.

Rotondo EK, Bieszczad KM (2021b) Memory Specific to Temporal Features of Sound Is Formed by Cue-Selective Enhancements in Temporal Coding Enabled by Inhibition of an Epigenetic Regulator. J Neurosci Off J Soc Neurosci 41:9192–9209.

Salinas E, Sejnowski TJ (2000) Impact of correlated synaptic input on output firing rate and variability in simple neuronal models. J Neurosci Off J Soc Neurosci 20:6193–6209.

Schneider DM, Woolley SMN (2013) Sparse and Background-Invariant Coding of Vocalizations in Auditory Scenes. Neuron 79:141–152.

Schreiner CE, Polley DB (2014) Auditory map plasticity: diversity in causes and consequences. Curr Opin Neurobiol 24:143–156.

Shang A, Bieszczad KM (2022) Epigenetic mechanisms regulate cue memory underlying discriminative behavior. Neurosci Biobehav Rev 141:104811.

Shang A, Bylipudi S, Bieszczad KM (2019) Inhibition of histone deacetylase 3 via RGFP966 facilitates cortical plasticity underlying unusually accurate auditory associative cue memory for excitatory and inhibitory cue-reward associations. Behav Brain Res 356:453–469.

Shilling-Scrivo K, Mittelstadt J, Kanold PO (2021) Altered Response Dynamics and Increased Population Correlation to Tonal Stimuli Embedded in Noise in Aging Auditory Cortex. J Neurosci 41:9650–9668.

Snyder JS, Alain C (2007) Toward a neurophysiological theory of auditory stream segregation. Psychol Bull 133:780–799.

Stefanko DP, Barrett RM, Ly AR, Reolon GK, Wood MA (2009) Modulation of long-term memory for object recognition via HDAC inhibition. Proc Natl Acad Sci U S A 106:9447–9452.

Studebaker GA, Sherbecoe RL, McDaniel DM, Gwaltney CA (1999) Monosyllabic word recognition at higher-than-normal speech and noise levels. J Acoust Soc Am 105:2431–2444.

Studer F, Barkat TR (2022) Inhibition in the auditory cortex. Neurosci Biobehav Rev 132:61–75.

Teschner MJ, Seybold BA, Malone BJ, Hüning J, Schreiner CE (2016) Effects of Signal-to-Noise Ratio on Auditory Cortical Frequency Processing. J Neurosci 36:2743–2756.

Weinberger NM (2004) Specific long-term memory traces in primary auditory cortex. Nat Rev Neurosci 5:279–290.

Wood KC, Blackwell JM, Geffen MN (2017) Cortical inhibitory interneurons control sensory processing. Curr Opin Neurobiol 46:200–207.

FIGURES

Figure 1.

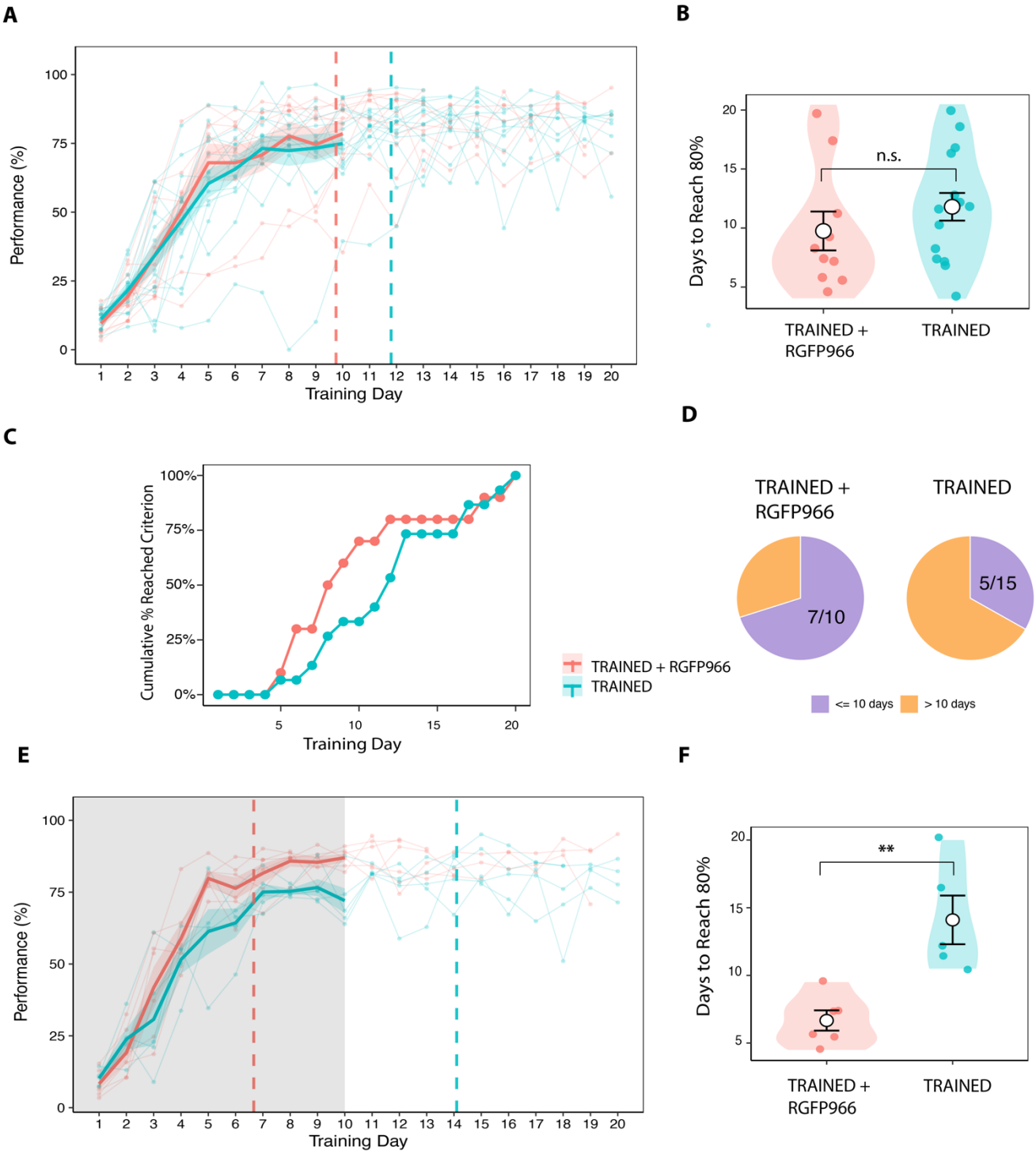

Figure 2.

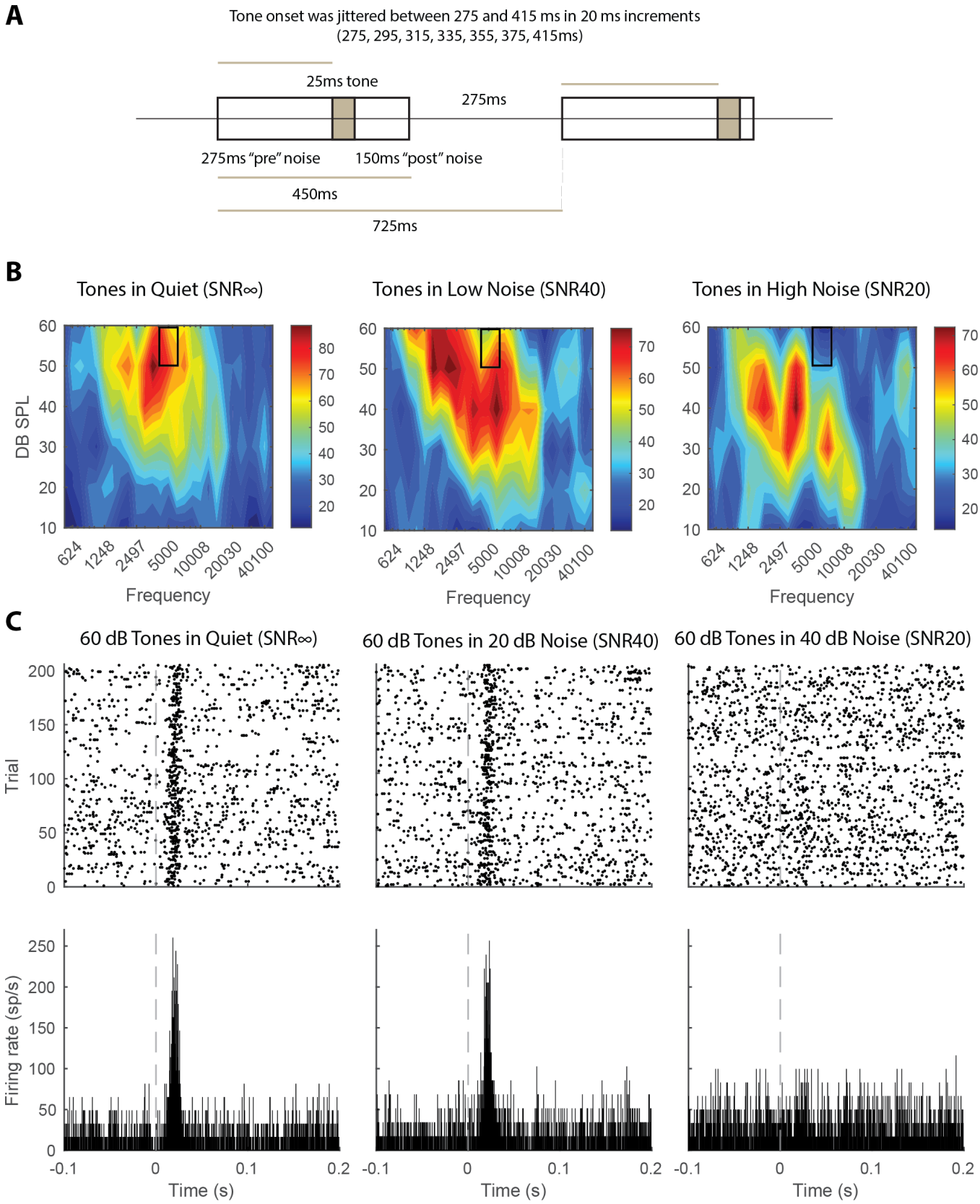
A
Tone onset was jittered between 275 and 415 ms in 20 ms increments
(275, 295, 315, 335, 355, 375, 415ms)
25ms tone
275ms
275ms "pre" noise
150ms "post" noise
450ms
725ms
B
Tones in Quiet (SNR∞)
Tones in Low Noise (SNR40)
Tones in High Noise (SNR20)
DB SPL
Frequency
624
1248
2497
5000
10008
20030
40100
C
60 dB Tones in Quiet (SNR∞)
60 dB Tones in 20 dB Noise (SNR40)
60 dB Tones in 40 dB Noise (SNR20)
Trial
Firing rate (sp/s)
Time (s)

Figure 3.

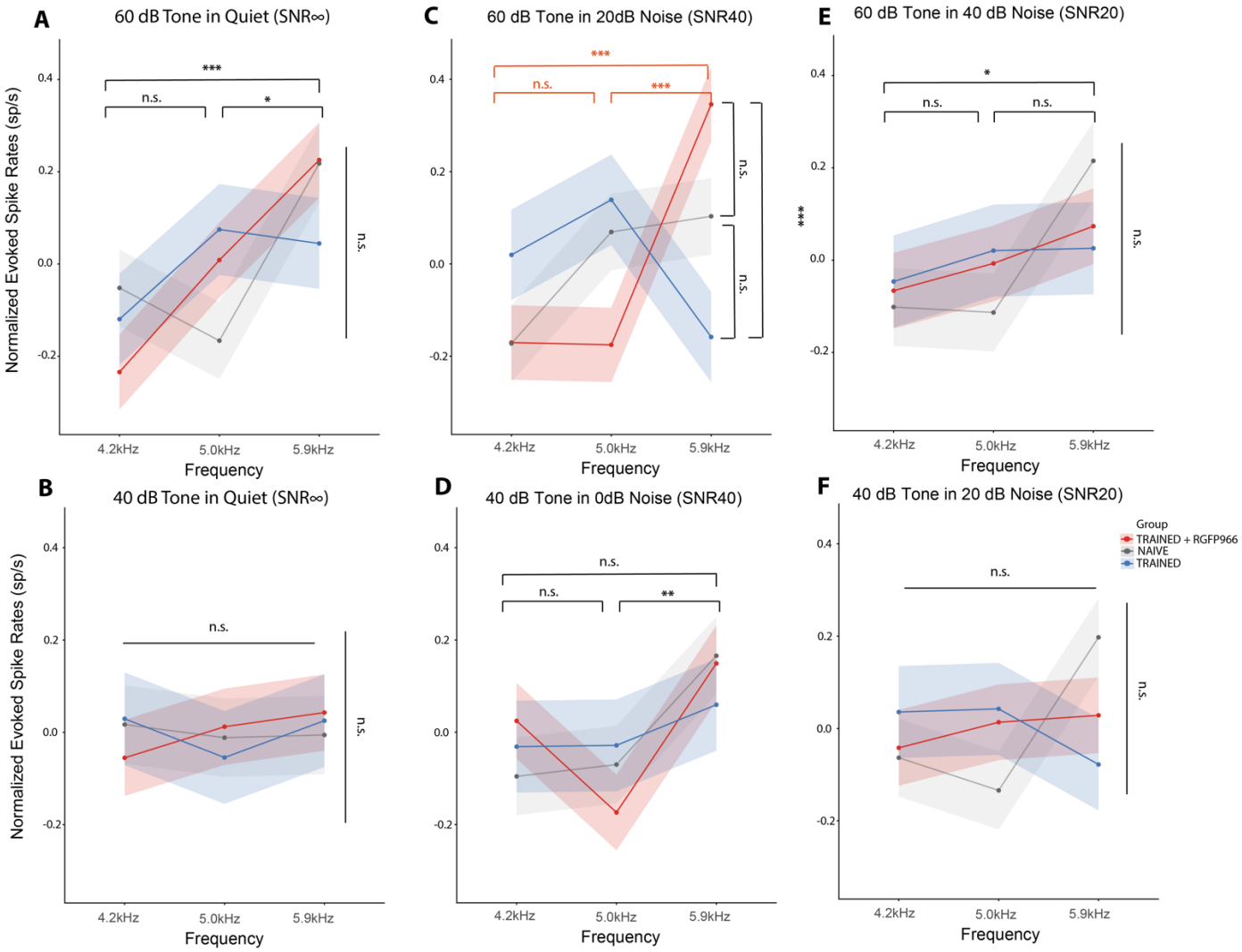
A
60 dB Tone in Quiet (SNR∞)
C
60 dB Tone in 20dB Noise (SNR40)
E
60 dB Tone in 40 dB Noise (SNR20)
B
40 dB Tone in Quiet (SNR∞)
D
40 dB Tone in 0dB Noise (SNR40)
F
40 dB Tone in 20 dB Noise (SNR20)
Normalized Evoked Spike Rates (sp/s)
Frequency
4.2kHz
5.0kHz
5.9kHz
n.s.
*
**
***
Group
TRAINED + RGFP966
NAIVE
TRAINED

Figure 4.

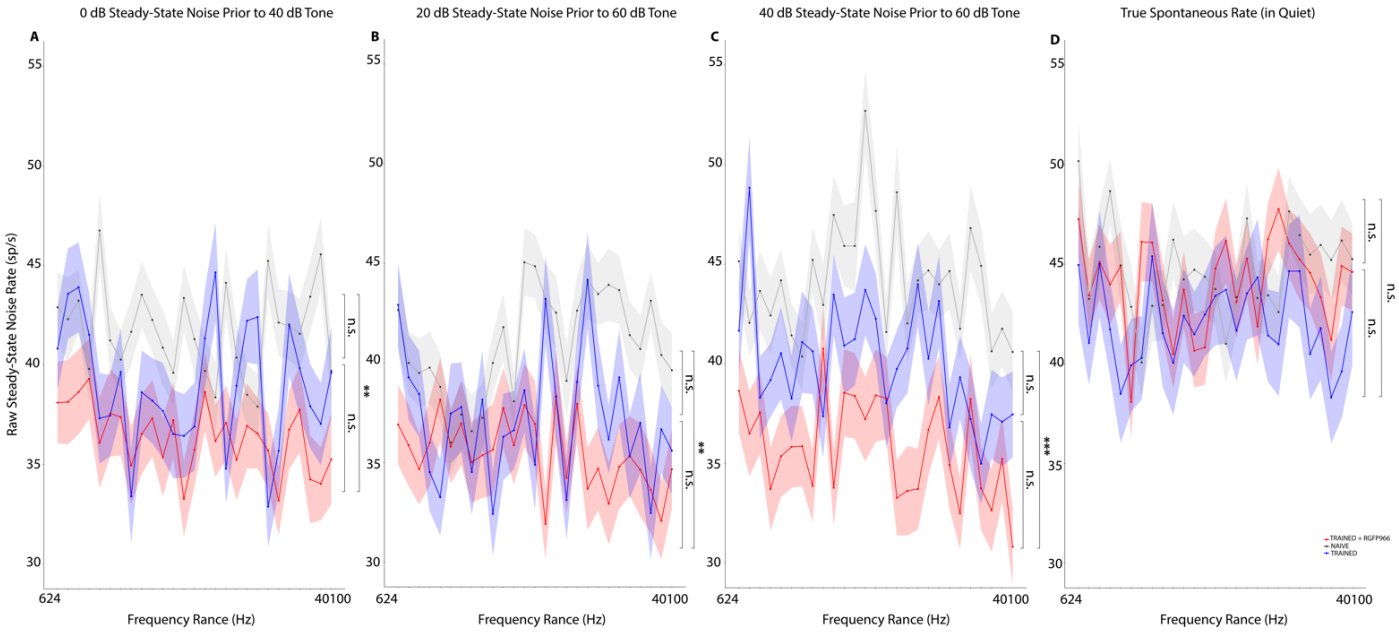

Figure 5.

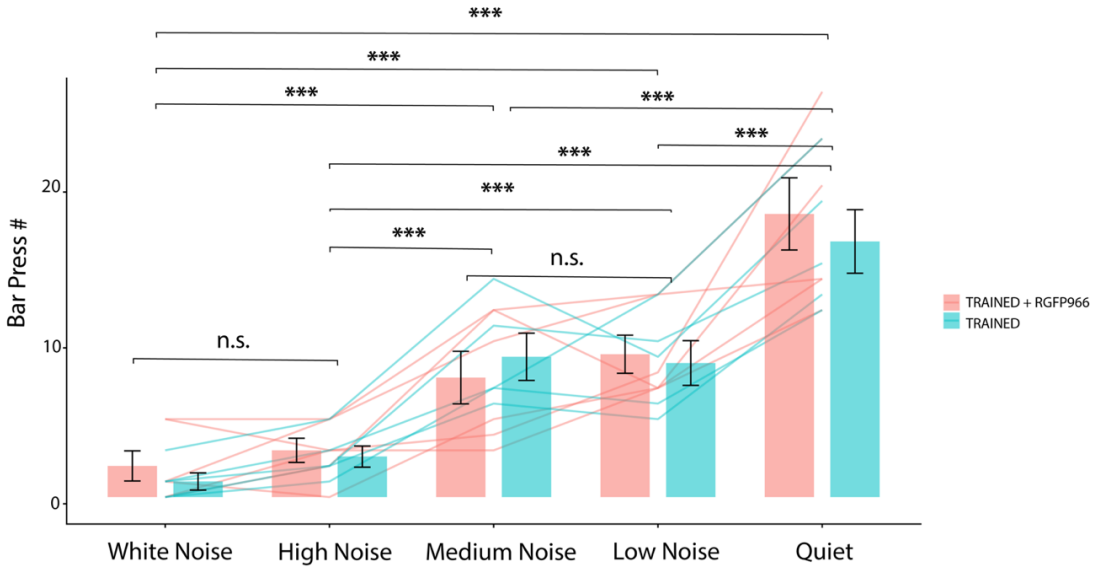

Figure 6.

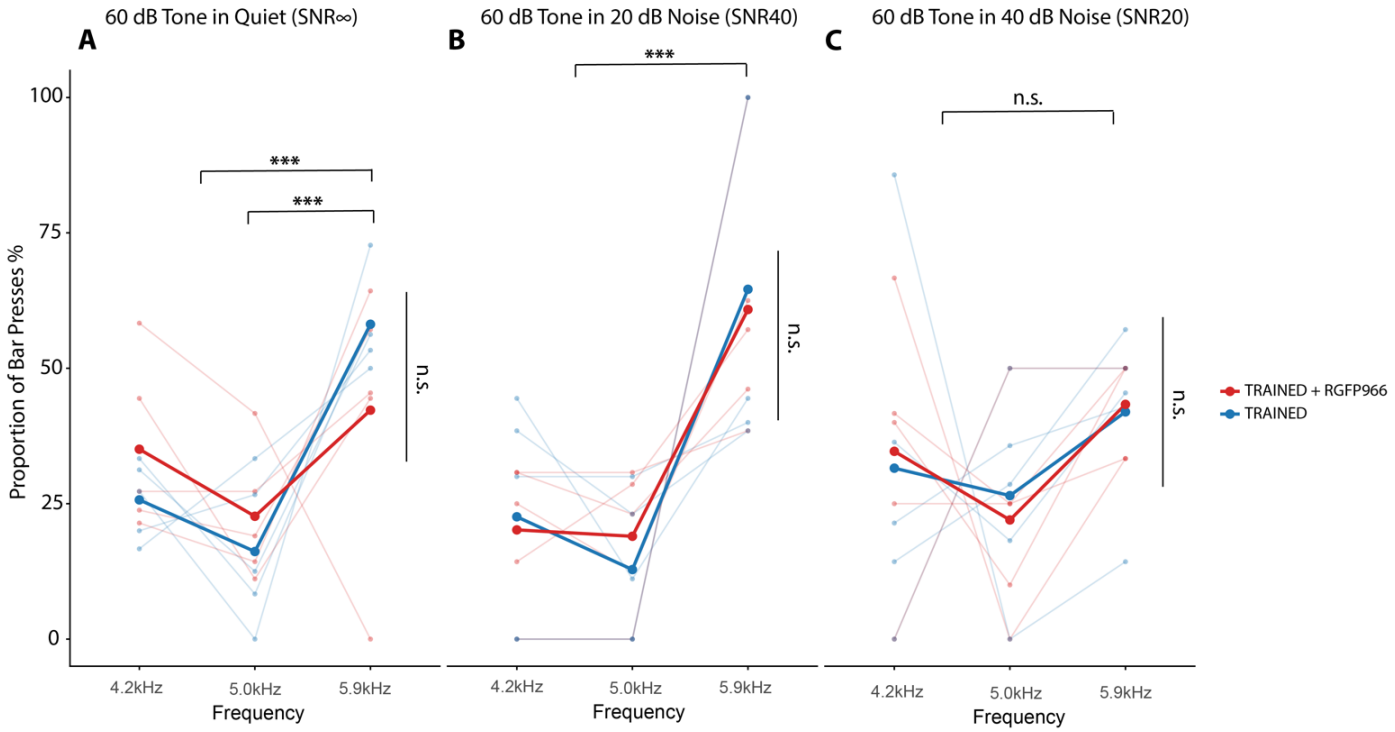
60 dB Tone in Quiet (SNR∞)
A
60 dB Tone in 20 dB Noise (SNR40)
B
60 dB Tone in 40 dB Noise (SNR20)
C
Proportion of Bar Presses %
100
75
50
25
0
***
***
n.s.
***
n.s.
n.s.
n.s.
4.2kHz
5.0kHz
5.9kHz
Frequency
TRAINED + RGFP966
TRAINED

Figure S1.

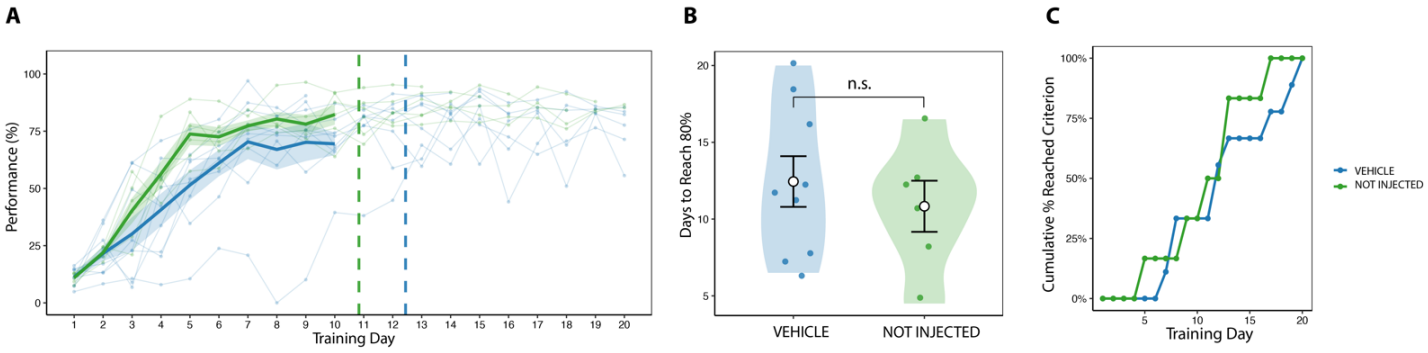

Figure S2.

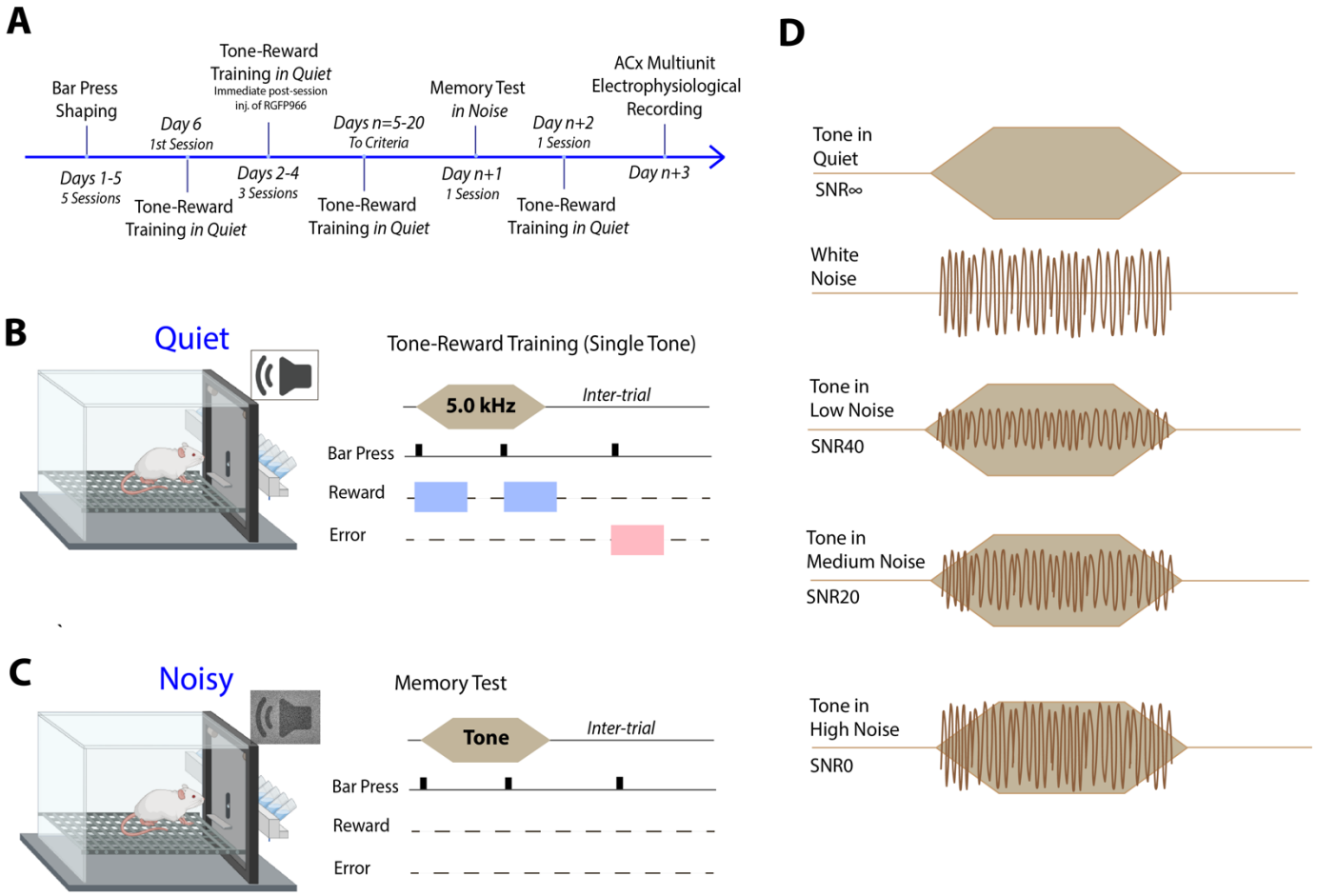

Figure S3.

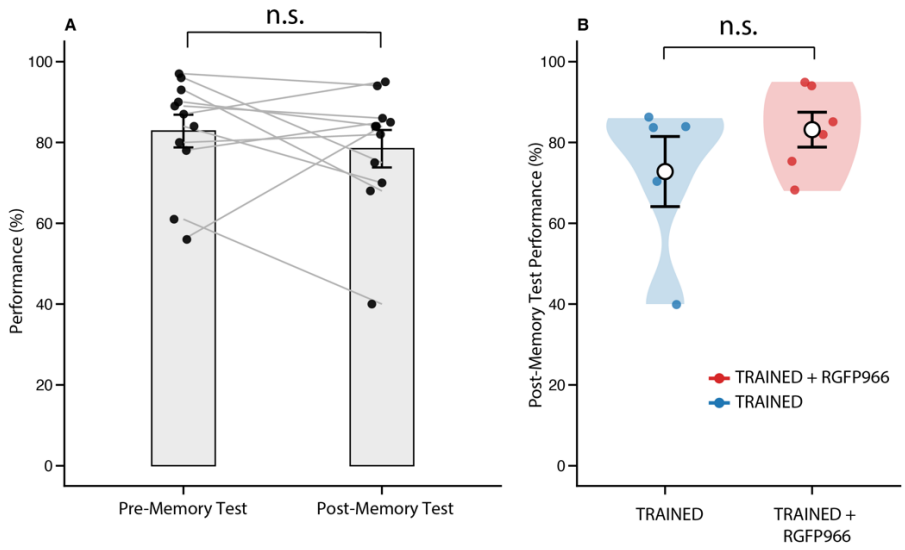
A
n.s.
Performance (%)
100
80
60
40
20
0
Pre-Memory Test
Post-Memory Test
B
n.s.
Post-Memory Test Performance (%)
100
80
60
40
20
0
TRAINED + RGFP966
TRAINED
TRAINED
TRAINED +
RGFP966